



Estimation of Road Loads and Vibration Transmissibility of Torsion Bar Suspension System in a Tracked Vehicle

G. P. S. Gagneza¹ · Sujatha Chandramohan²

Received: 22 December 2017 / Accepted: 12 April 2018 / Published online: 18 May 2018
© The Institution of Engineers (India) 2018

Abstract Designing the suspension system of a tracked combat vehicle (CV) is really challenging as it has to satisfy conflicting requirements of good ride comfort, vehicle handling and stability characteristics. Many studies in this field have been reported in literature and it has been found that torsion bars satisfy the designer's conflicting requirements of good ride and handling and thus have reserved a place for themselves as the most widely used suspension system for military track vehicles. Therefore, it is imperative to evaluate the effectiveness of the torsion bar under dynamic conditions of undulating terrain and validating the same by correlating it with computer simulation results. Thus in the present work, the dynamic simulation of a 2N + 4 degrees of freedom (DOF) mathematical model has been carried out using MATLAB Simulink and the vibration levels were also measured experimentally on a 12 wheel stationed high mobility military tracked infantry combat vehicle (ICV BMP-II) traversing different terrain, that is, Aberdeen proving ground (APG) and Sinusoidal, at a constant vehicle speed. The dynamic force transmitted to the hull CG through the 12 torsion bar suspension systems was computed to be around 26,700 N and found to match the measured values. The vibration isolation of the torsion bar in bounce was found to be effective, with a transmissibility from the road wheel to the hull of about 0.6.

Keywords Tracked combat vehicle · Ride dynamics · MATLAB Simulink · Torsion bar

Notations

a_i	Longitudinal distance of i th road wheel from CG
b_i	Lateral distance of i th road wheel from CG
C_{di}	Damping coefficient for i th wheel
C_{seat}	Damping coefficient for driver's seat
I_p	Pitch moment of inertia
I_r	Roll moment of inertia
I_y	Half pitch moment of inertia
K_{seat}	Stiffness of driver's seat
K_{tbi}	Stiffness of i th torsion bar
K_{wi}	Stiffness of i th road wheel
m_h	Half hull sprung mass
M_h	Hull sprung mass
T_{ri}	Track tension
X	Longitudinal axis
Y	Lateral axis
Z	Vertical axis
\ddot{Z}_h	Vertical acceleration response of hull
\dot{Z}_h	Vertical vibration velocity of hull
Z_h	Bounce motion of hull
\ddot{z}_{wi}	Vertical acceleration response of i th road wheel station
\dot{z}_{wi}	Vertical velocity of i th road wheel station
Z_{wi}	Bounce motion of i th road wheel station
Z_{ri}	Road input to i th road wheel
θ	Pitch (about Y-axis)
θ	Pitch of hull CG
φ	Roll (about X-axis)
φ	Roll of hull CG
Φ	Yaw (About Z-axis)

✉ Sujatha Chandramohan
sujatha@iitm.ac.in

¹ Indian Army, New Delhi, India

² Machine Design Section, Department of Mechanical Engineering, Indian Institute of Technology Madras, Chennai 600036, India

Introduction

Military tracked combat vehicles (CVs) are designed to sustain severe vibration as operational requirements necessitate their exploitation in ride over rough terrain. The dynamic response of a CV during a cross-country run, which is a random terrain input, has been of major design concern to automotive engineers for many years. This concern arises from the fact that excessive levels of vibrations can lead to ride discomfort, ride safety problems as well as dynamic stressing in vehicle frame and suspension components. To overcome these problems, designing a suspension system becomes critical in improving ride comfort and safety. Thus, the suspension system is designed with the objective of reducing the vibration to the personnel and load being borne by the vehicle, the advantage being reduced driver fatigue and reduced harm to the vehicle. The suspension keeps the wheel in contact with the ground; the higher the deflection, the greater the force that the spring applies according to its stiffness. The stiffer the spring, the harsher the ride and less comfortable passengers are, but better the handling capabilities. Therefore, suspension design is a constant tradeoff between handling and ride comfort. Many studies in this field were carried out and it was found that torsion bars satisfy these conflicting requirements and are the most widely used suspension system for military track vehicles.

Hohl [1] delineated the features of torsion-bar spring and damping systems, which are widely used in military tracked vehicle suspension system. Rakheja et al. [2] proposed a tank model considering the suspension system, track-terrain interactions, track tension and stiffness of the track pad to study ride characteristics of a military tracked vehicle fitted with torsion bar suspension system. The military tracked vehicle model had a trailing arm torsion bar suspension system; analysis of ride characteristics was done using a nonlinear vehicle model. The ride quality analysis of the said vehicle was carried out by finding average absorbed power. Dhir and Sankar [3] have carried computer simulation and field trials on ride dynamics of high mobility wheeled/tracked off-road vehicles considering the track tension, terrain undulations and stiffness of the track pad while traversing rough off road terrain. Dhir and Sankar [4] developed an in-plane ride model to compare the ride performance of a torsion bar suspension system with a hydrogas suspension system. Sujatha et al. [5] developed a half car model ($N + 2$) of a tracked vehicle and analyzed the same considering the bounce and pitch motions of the sprung mass and vertical motion of each road wheel as a degree of freedom (DOF). Yamakawa and Watanabe [6] did a spatial motion analysis of a tracked vehicle with independent torsion bar type suspension in

order to numerically simulate the motion of the vehicle including the road wheels. The said model reasonably predicted the motion of the tracked vehicle with torsion bar type suspension and the same was established by comparing numerical analysis with experiments on a scaled model. Baokun [7] developed a multibody dynamics model of a tracked vehicle fitted with torsion bar suspension system to study ride comfort and safety. Kadir et al. [8] developed a 2 DOF tracked vehicle model using MATLAB Simulink and studied the vertical motions of the sprung and unsprung masses to a known road input. They also compared the results with experiments on the model.

Objectives of the Present Work

Analytical studies with emphasis on transmissibility of the torsion bar suspension in bounce and determination of road loads have not been reported in literature. Hence in the present work, dynamic analysis of a high mobility tracked vehicle was carried out with the following objectives:

1. To conduct studies on a CV with torsion bar suspension system by performing dynamic tests on the vehicle on defined tracks: (a) Sinusoidal and (b) Aberdeen proving ground (APG) at constant speed and to study the same analytically using $2N + 4$ DOF CV model in MATLAB Simulink.
2. To estimate the road loads transferred to the hull through the road wheels through experiment and analysis.
3. To determine the vibration transmissibility characteristics of the torsion bar in bounce through experiment and analysis.

All experiments and simulation studies have been carried out at a constant vehicle speed of 15 kmph and analyses are done using a linear model. Parameters of the CV (that is, torsion bar stiffness and damping coefficient) used in the model are assumed to be constant.

Eigenvalue Analysis of Tank

To carry out the dynamic analysis, a $2N + 4$ DOF full car mathematical model was developed. In the model, $2N$ DOF correspond to the bounce motion of the $2N$ road wheels and 4 DOF correspond to the roll, pitch and bounce motions of the sprung mass CG and driver seat bounce motion. Prior to that the torsion bar stiffness and shock absorber damping characteristics have been computed. The ICV has been fitted with 12 torsion bars. A sketch of the torsion bar is shown in Fig. 1a and locations of dampers are shown in Fig. 1b. Each torsion bar is attached to a wheel at one end, whereas the other end is splined to the hull.

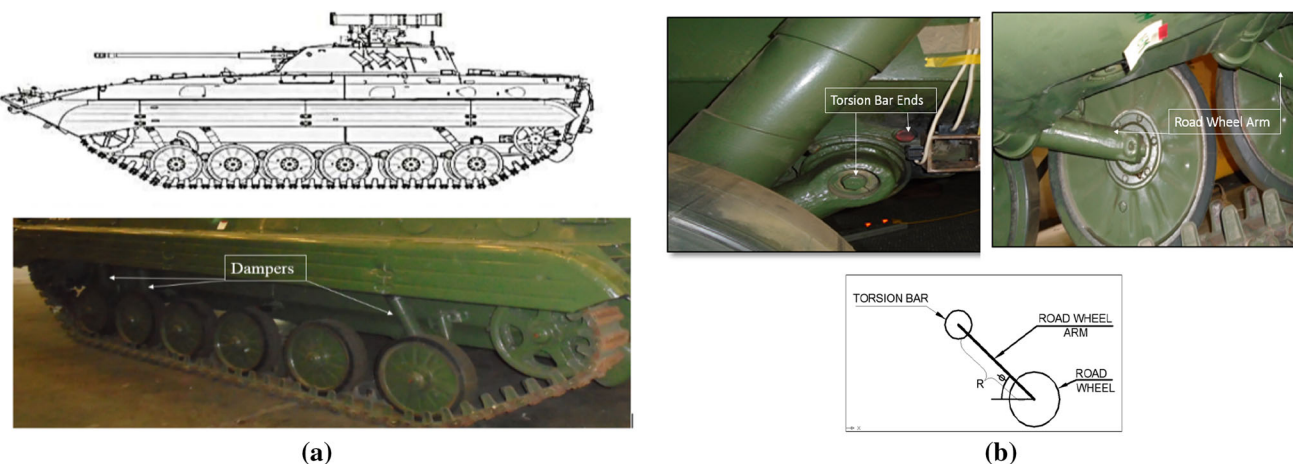


Fig. 1 **a** Schematic of torsion bar **b** locations of dampers

Wheel Rate of Torsion Bar Stiffness (K_{tb})

The procedure for computation of torsion bar stiffness and shock absorber damping used in the analytical model is described here. The torsion bar is a linear spring for twist angles of the order of 40° over the operating range considered. For the computation, the angle between the road wheel arm and the horizontal line is that at the free position of the torsion bar (without the application of any torque). Suspension stiffness is the ratio of the vertical force acting on the road wheel to the corresponding vertical displacement. Though this is found to be slightly non-linear, the suspension stiffness can be taken as constant and equal to its average value [9].

$$\text{Torsional stiffness of torsion bar} = \frac{T}{\theta} = \frac{GJ}{l} = \frac{G\pi d^4}{32l} \quad (1)$$

$$\begin{aligned} \text{Wheel rate of stiffness} = K_{tb} &= \frac{T}{\theta} \left(\frac{1}{R \cos \phi} \right)^2 \\ &= \frac{\pi d^4 G}{32 l R^2 (\cos \phi)^2} \end{aligned} \quad (2)$$

where d = diameter of torsion bar = 0.038 m; G = modulus of rigidity of steel = 84×10^9 N/m 2 ; l = length of torsion bar = 2.075 m; R = length of road wheel arm = 0.325 m and Φ = angle between road wheel arm and horizontal line = 30° as seen from Fig. 1a.

On calculating, torsion bar stiffness, K_{tb} is found to be 75,530 N/m.

Estimation of Shock Absorber Damping Characteristics (C_d)

The ICV BMP-II has been fitted with three dampers each, on both sides of the vehicle, that is, at wheel sets 1, 2 and 6. Wheel rate of damping

$$C_d = C_c N^2 \quad (3)$$

where damping coefficient $C_c = 70,000$ Ns/m and α = angle between shock absorber axis and road wheel arm. The damping characteristics of three wheel stations 1, 2 and 6 for 40 mm stroke are as shown in Table 1.

Eigenvalue Problem

To carry out dynamics analysis, a $2N + 4$ DOF full car mathematical model was developed. Figure 2 shows the coordinates associated with CV. In the model, 4 DOF correspond to the roll (ϕ), the pitch (θ), the bounce (Z_h) motion of the sprung mass CG and driver seat bounce (Z_{seat}) motion, while $2N$ DOF correspond to bounce motion of road wheels as shown in Fig. 2.

The general equations of motion for eigenvalue analysis can be given as

$$[M]\{\ddot{z}\} + [C]\{\dot{z}\} + [K]\{z\} = \{0\} \quad (4)$$

This equation can be rewritten in the form of a non-standard eigenvalue problem:

$$[K]\{z\} = \omega^2[M]\{z\} \quad (5)$$

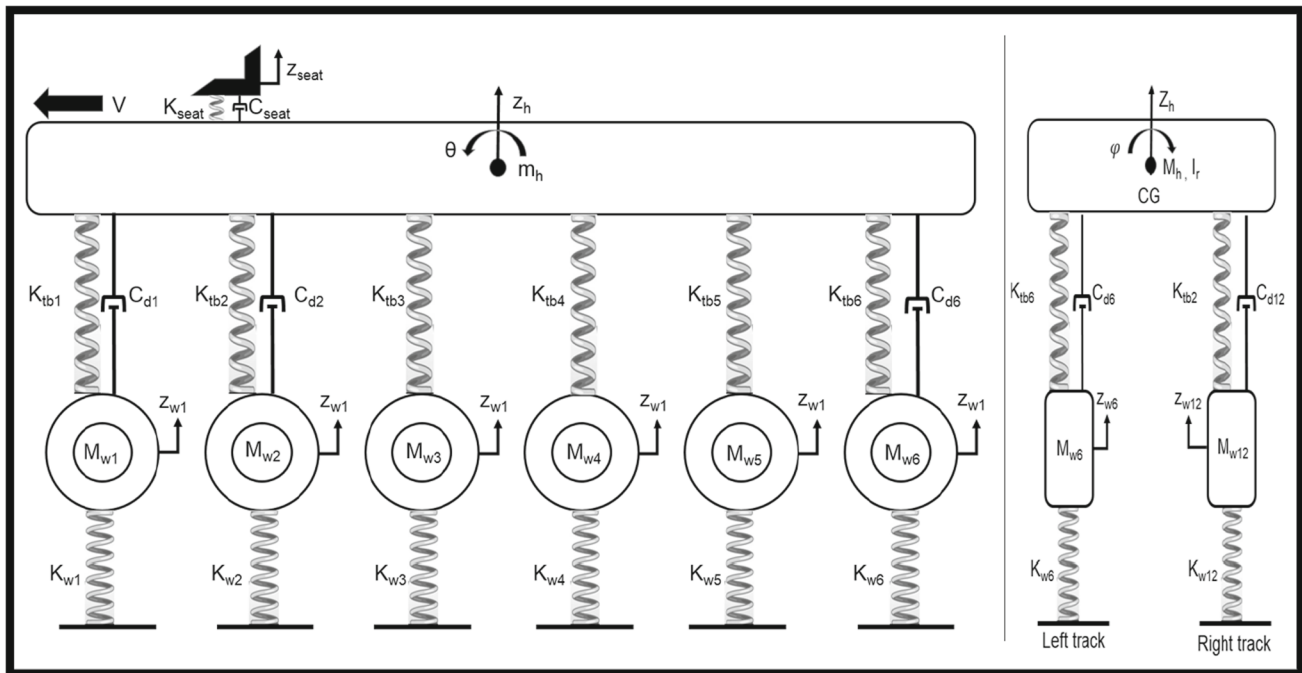
where $[M]$ is the mass matrix; $[C]$ is the damping matrix (which is neglected while obtaining eigenvalues) and $[K]$ is the stiffness matrix; $\{z\}$ is the displacement vector.

The generalized equation for hull bounce, hull pitch and hull roll at CG are as given here.

$$\begin{aligned} M_h \ddot{Z}_h + C_{di} (\dot{Z}_h + a_i \dot{\theta} + b_j \dot{\phi} - \dot{z}_{wi}) \\ + K_{tbi} (Z_h + a_i \theta + b_j \phi - z_{wi}) \\ - C_{seat} (\dot{Z}_{seat} - (\dot{Z}_h + a_i \dot{\theta} + b_j \dot{\phi})) \\ - K_{seat} (Z_{seat} - (Z_h + a_i \theta + b_j \phi)) = 0 \end{aligned} \quad (6)$$

Table 1 Damping characteristics C_d for 40 mm stroke

For 1st and 2nd wheel stations	For 6th wheel station
$\theta = 30^\circ; \alpha = 36^\circ; a = 0.125 \text{ m}$	$\theta = 30^\circ; \alpha = 15^\circ; a = 0.125 \text{ m}$
Suspension ratio (N) = $\frac{(a \sin \alpha)}{R \cos \theta} = \frac{(0.125) \sin 36}{(0.325) \cos 30} = 0.26$	Suspension ratio (N) = $\frac{(a \sin \alpha)}{R \cos \theta} = \frac{(0.125) \sin 15}{(0.325) \cos 30} = 0.115$
Wheel rate of damping coefficient, Ns/m	
In compression 4732	925.75
In tension 690.93	231.44

**Fig. 2** 2N + 4 full car model of ICV BMP-II

$$I_p \ddot{\theta} + C_{di} (\dot{Z}_h + a_i \dot{\theta} + b_j \dot{\phi} - \dot{z}_{wi}) a_i + K_{tbi} (Z_h + a_i \theta - z_{wi} + b_j \varphi) a_i - C_{seat} (\dot{Z}_{seat} - (\dot{Z}_h + a_i \dot{\theta} + b_j \dot{\phi})) a - K_{seat} (Z_{seat} - (Z_h + a_i \theta + b_j \varphi)) a = 0 \quad (7)$$

$$I_r \ddot{\phi} + C_{di} (\dot{Z}_h + a_i \dot{\theta} + b_j \dot{\phi} - \dot{z}_{wi}) b + K_{tbi} (Z_h + a_i \theta + b_j \varphi - z_{wi}) b + C_{seat} (\dot{Z}_{seat} - (\dot{Z}_h + a_i \dot{\theta} + b_j \dot{\phi})) b + K_{seat} (Z_{seat} - (Z_h + a_i \theta + b_j \varphi)) b = 0 \quad (8)$$

The generalized equation for individual wheel bounce is as given here.

$$M_{wi} \ddot{z}_{wi} - C_{di} (\dot{Z}_h + a_i \dot{\theta} + b_j \dot{\phi} - \dot{z}_{wi}) - K_{tbi} (Z_h + a_i \theta + b_j \varphi - z_{wi}) + K_{wi} (z_{wi}) - T_{ri} = K_{wi} (z_{ri}) \quad (9)$$

Table 2 Parameters of the test vehicle (ICV BMP-II) used in the dynamic analysis

Hull Sprung mass (M_h)	10,250 kg
Pitch moment of inertia (I_p)	29,261.40 kg m ²
Roll moment of inertia (I_r)	7659.46 kg m ²
Mass of the road wheel 1, 5 and 6 (m_{w1} , m_{w5} and m_{w6})	145.07 kg
Mass of the road wheel 2, 3 and 4 (m_{w2} , m_{w3} and m_{w4})	398.7 kg
Stiffness of road wheel (K_{wi})	75,530 N/m
Stiffness due to track tension (K_{tb})	65,672 N/m
Stiffness of torsion bar (K_{tbi})	75,530 N/m
Damping coefficient for wheels 1 and 2 (C_{d1} and C_{d2})	4732 Ns/m
Damping coefficient for wheel 6 (C_{d6})	925.75 Ns/m

where T_{ri} and Z_{ri} stand for track tension and road input for the i th wheel.

Table 3 Wheel longitudinal / lateral distance from CG

Road wheel set	Longitudinal / lateral distance of wheel from CG, m			
First set	1st road wheels, a_1	1.575	7th road wheels, a_7	1.665
Second set	2nd road wheels, a_2	0.9	8th road wheels, a_8	0.99
Third set	3rd road wheels, a_3	0.25	9th road wheels, a_9	0.34
Fourth set	4th road wheels, a_4	0.4	10th road wheels, a_{10}	0.31
Fifth set	5th road wheels, a_5	1.160	11th road wheels, a_{11}	1.07
Sixth set	6th road wheels, a_6	1.885	12th road wheels, a_{12}	1.795
Left track wheels, m, b_l				1.275
Right track wheels, m, b_r				1.275

Table 4 Natural frequencies of the tank estimated using $2N + 4$ full car model

Mode	Estimated natural frequencies, Hz
Sprung mass bounce frequency	2.38
Sprung mass pitch frequency	1.42
Sprung mass roll frequency	0.82
Driver Seat Bounce frequency	2.25
1st wheel station bounce frequency	14.43
2nd wheel station bounce frequency	16.36
3rd wheel station bounce frequency	16.88
4th wheel station bounce frequency	15.91
5th wheel station bounce frequency	15.23
6th wheel station bounce frequency	13.89
7th wheel station bounce frequency	14.43
8th wheel station bounce frequency	16.36
9th wheel station bounce frequency	16.88
10th wheel station bounce frequency	15.91
11th wheel station bounce frequency	15.23
12th wheel station bounce frequency	13.89

The eigenvalue analysis has been performed using MATLAB. Parameters used for the analysis are shown in Tables 2 and 3. Estimated natural frequencies are shown in Table 4.

Experimental Trials on Sinusoidal and APG Tracks

Extensive experimental trials were carried out to estimate the road loads transferred by the torsion bars and their transmissibility in bounce.

Static Test

In order to understand the road loads transferred to the hull, it has been assumed that the strains measured near the torsion bar anchors are indicative of the road loads transferred. Therefore a static loading and unloading test was carried out to measure the strain corresponding to the load on a wheel station. Strain gauges FCA-6-11 (TML, Japan) were pasted near the wheel station as shown in Fig. 3a in half bridge configuration with one active gauge and a dummy gauge and the signals were conditioned and acquired using Quantum X data acquisition system (HBM, Germany). To obtain the load values from the strain gauge readings, the CV was lifted up slowly from the ground using an overhead crane such that the entire weight of the CV was carried by the crane as shown in Fig. 3b and then fully lowered to the ground, with the strains being recorded for both cases.



(a)



(b)



(c)

Fig. 3 a Strain gauge b CV lifted by overhead crane to calibrate strain c measuring load on a weigh bridge

Dynamic vertical load acting on each wheel station was also measured by using a weighbridge (Fig. 3c). Measurements were made in such a manner that only the first set of wheel stations was on the weighbridge and the remaining wheels were on the ground and the corresponding load was recorded. Then the 2nd wheel station set was moved on to the weighbridge and the combined load of 1st and 2nd wheel stations was recorded. The value for the 2nd wheel set could be calculated by subtracting the value corresponding to the 1st wheel set from the second reading. Similarly the load distribution on the other wheel station sets was measured sequentially. Table 5 shows the measured strain values at wheel station 4 and Table 6 the load carried by each wheel station. Tables 5 and 6 indicate that the 4th wheel station alone carries 14,028 N load of the CV and this corresponds to 48.32 $\mu\text{m}/\text{m}$ strain.

Experimental Setup for Dynamic Measurements

Dynamic trials were carried out at a constant speed of 15 kmph to measure the response of the tank near the six wheel stations and on the sprung mass (hull plus turret) CG in

the vertical direction. Acceleration responses were measured on the two tracks (a) Sinusoidal track and (b) APG track, as shown in Fig. 4a, b. Sinusoidal track with pitch 7 m and peak amplitude 0.1 m is made of concrete. The APG track consists of bumps of different heights arranged in a random manner. Details regarding these test tracks are shown in the “[Appendix](#)”. MEMS accelerometers SAA-1150-1000 (NeuWGhent Technology, USA) were used for vertical acceleration response measurement near all the wheel stations and the driver's seat. Since the accelerometers could not be attached directly to the wheels, they were mounted near the wheel stations at the locations where the wheel arms are rigidly fastened to the hull of the vehicle as shown in Fig. 4c. Six DOF accelerometers / rate gyros TANS-3115010M5-25100 (NeuWGhent Technology, USA) were fixed at the hull CG. DEWE 501-Dewetron logger was used for data acquisition. The power required for measurements was obtained through a 12 V battery and inverter.

Dynamic Forces Transmitted to Hull CG

Strain values measured near the 4th wheel station on the Sinusoidal track are shown in Fig. 5a. These dynamic strains were then calibrated as per the data mentioned in Table 6 to get the dynamic load acting on the vehicle under running condition and the corresponding calibrated loads are shown in Fig. 5b. From Tables 5 and 6, it is seen that the 4th wheel station carries 14,028 N load of the CV and this corresponds to 48.32 $\mu\text{m}/\text{m}$ strain. From Fig. 5a, the peak strain value is 92 $\mu\text{m}/\text{m}$. Therefore, force F_T transmitted to the hull = $(14,028 / 48.32) \times 92 = 26,708.94$ N. In Fig. 5b, the load is shown by converting the strain using the above calibration factor; the peak force transmitted is 26,708.94 N.

In order to compute the dynamic forces acting at the hull CG and validate the above measured values, the basic

Table 5 Strains measured at wheel station 4

Condition	Strain, $\mu\text{m}/\text{m}$
Fully lifted (no load)	0
Fully grounded	48.32

Table 6 Load distribution of the tracked vehicle

Wheel station	Load carried by each wheel, N	Wheel station	Load carried by each wheel, N
1	4022	4	14,028
2	13,980	5	10,300
3	16,628	6	1815



Fig. 4 a Sinusoidal track b APG track c MEMS accelerometers

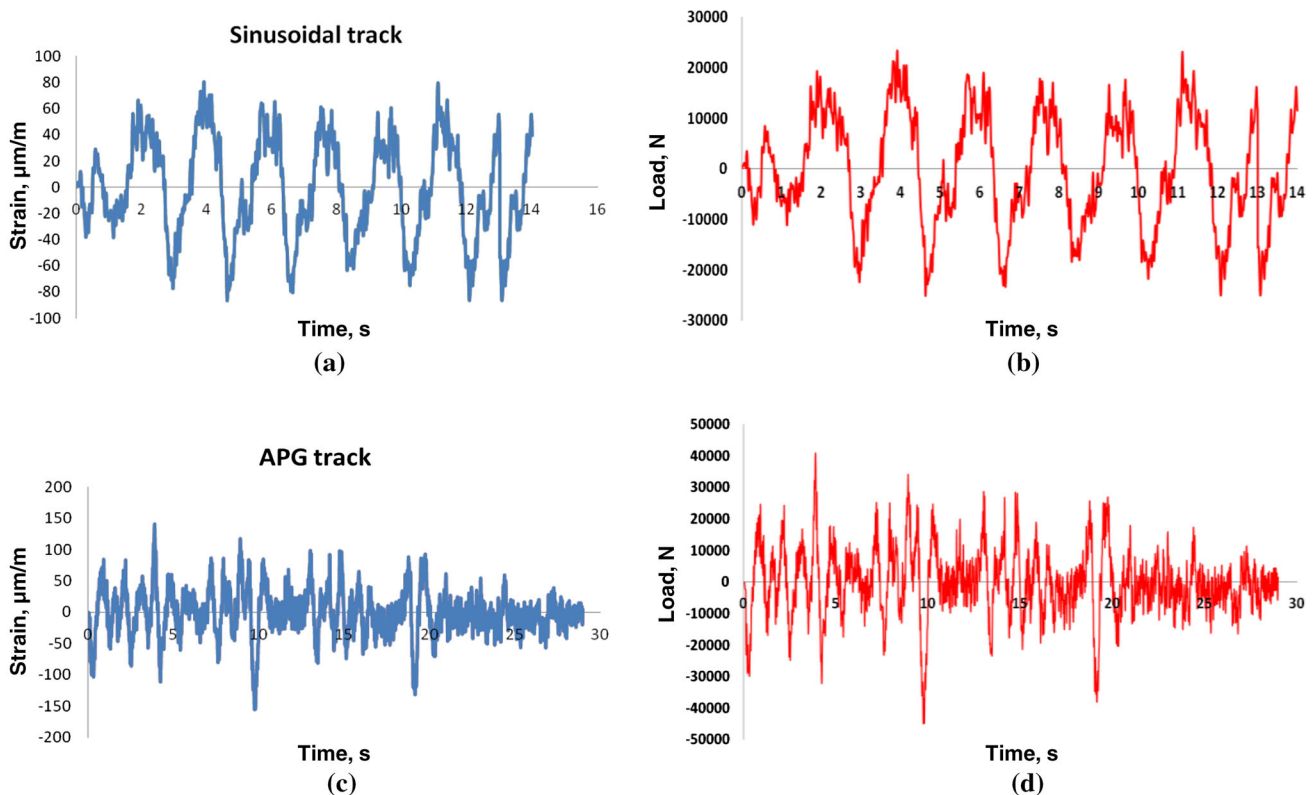


Fig. 5 **a** Time record of strain value measured near 4th wheel station on Sinusoidal track. **b** Dynamic vertical load acting on 4th wheel station on Sinusoidal track. **c** Time record of strain value measured

near 4th wheel station on APG track. **d** Dynamic vertical load acting on 4th wheel station on APG track

equation for peak force transmitted from the 12 road wheels is

$$F_T = \sqrt{12(K^2Y^2) + 6(\omega^2C^2Y^2)} \quad (10)$$

where $\omega = 2\pi f = 3.7385$ rad/s; frequency (f) = $\frac{v}{\lambda} = \frac{4.1667}{7} = 0.595$ Hz; wavelength (λ) = 7 m; velocity (v) = 4.1667 m/s and peak amplitude = 0.1 m.

Equation (10) is formulated considering the fact that the CV has 12 torsion bars and six dampers.

Therefore,

$$\begin{aligned} F_T &= \sqrt{12(75530^2 \times 0.1^2) + 3.7385^2(4 \times 4732^2 + 2 \times 925.75^2)0.1} \\ &= 26647.52 \text{ N} \end{aligned}$$

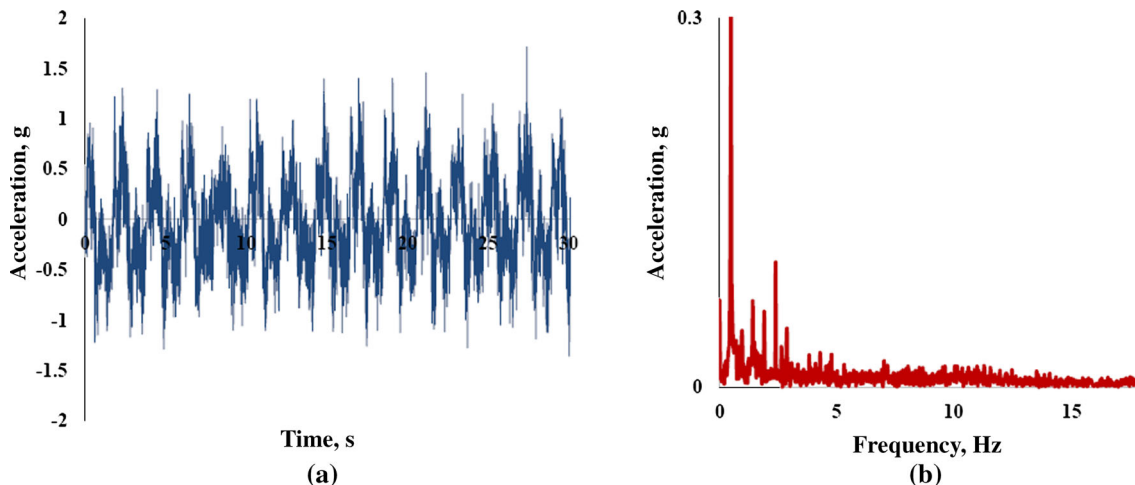


Fig. 6 **a** Time record of acceleration at wheel station 2 in vertical direction on Sinusoidal track. **b** Spectrum of acceleration at wheel station 2 in vertical direction on Sinusoidal track

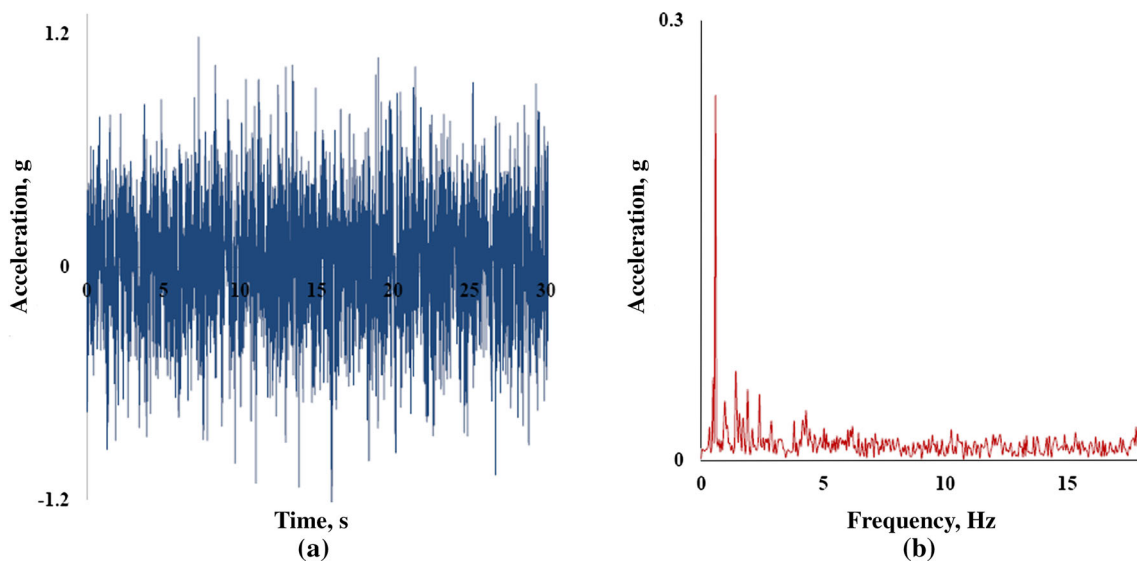


Fig. 7 **a** Time record of acceleration at hull CG in vertical direction on Sinusoidal track. **b** Spectrum of acceleration at hull CG in vertical direction on Sinusoidal track

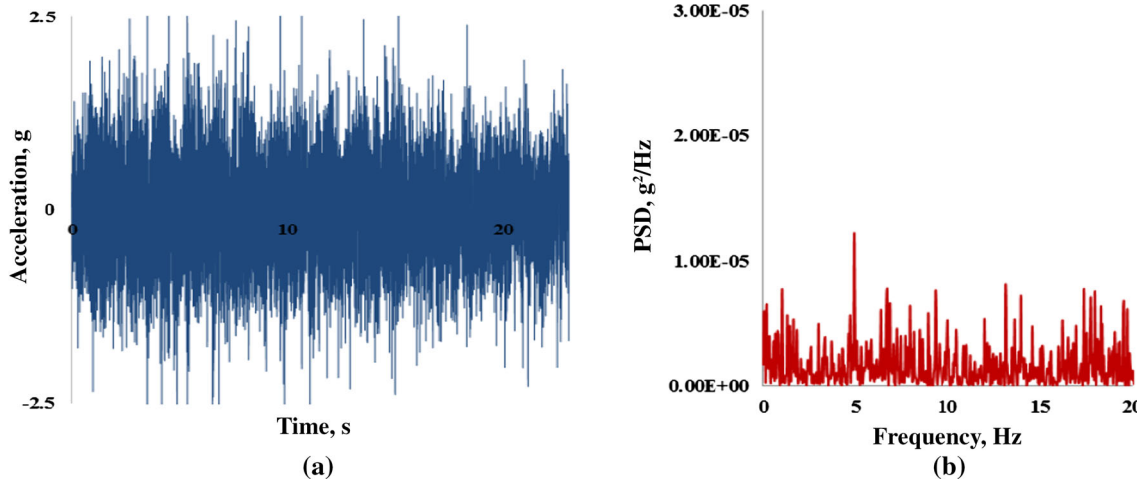


Fig. 8 **a** Time record of acceleration at wheel station 2 in vertical direction on APG track. **b** Spectrum of acceleration at wheel station 2 in vertical direction on APG track

This matches well with the value calculated using Eq. (10), that is, 26,708.94 N, as shown in Fig. 5b.

Having validated the road loads for the Sinusoidal terrain, the loads for the APG terrain were calculated. Figure 5c, d shows the measured strain and estimated load for the APG track.

Dynamic Test Results

Vertical acceleration measurements at all the wheel stations, sprung mass CG and driver's seat were recorded on Sinusoidal and APG tracks. A sample time record of vertical acceleration on the road wheel (Station 2) on Sinusoidal track is as shown in Fig. 6a. The corresponding spectrum is shown in Fig. 6b. Figure 7a, b shows the accelerations at the hull CG

while traversing the Sinusoidal track. Figure 8a shows a sample time record of vertical acceleration on the road wheel (Station 2) on APG track and Fig. 8b shows the corresponding power spectral density (PSD). Figure 9a, b shows the accelerations in the time domain and the PSD, respectively, at the hull CG while traversing the APG track. The accelerations are highest at the first wheel station and are higher for traversal on the APG track than the Sinusoidal track.

Dynamic Simulation using MATLAB-Simulink and Comparison with Experiment

Equations of motion for the $2N + 4$ DOF model of ICV BMP-II are incorporated into the SIMULINK application in state space form. The CV parameters as discussed in

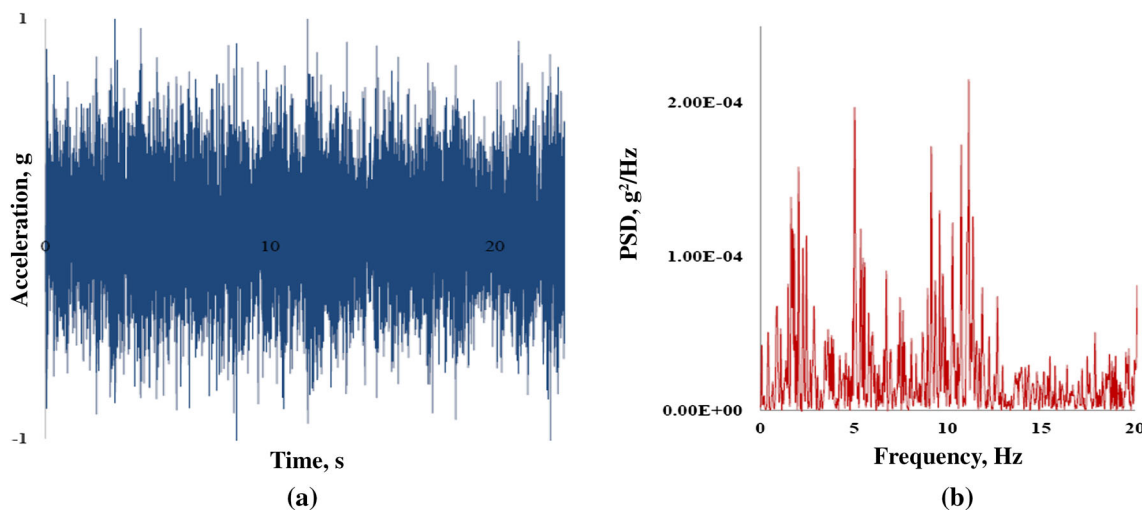


Fig. 9 **a** Time record of acceleration at hull CG in vertical direction on APG track. **b** PSD of acceleration at hull CG in vertical direction on APG track

Tables 2 and 3 have been utilised while modelling a full car model in Simulink.

Simulink Full Car Model

A schematic of the full car model is shown in Fig. 10.

Simulation Results

Vertical acceleration responses in time domain as well as in frequency domain corresponding to all the wheel stations, sprung mass CG and driver's seat were generated using MATLAB Simulink. A sample time record and spectrum of vertical acceleration on the road wheel (station 2) on Sinusoidal track are as shown in Fig. 11a, b.

Comparison of Experimental and Analytical Responses

Comparison of responses recorded from analytical studies (red lines) with experimental studies (blue lines) on Sinusoidal track are shown in Fig. 12 for wheel station 2. Figure 13 shows a comparison between experimental and analytical time records of vertical acceleration at wheel station 2 on an APG track. The difference between the measured time histories and calculated wheel accelerations are because the measured values are from the actual system with a very large number of DOF, whereas the computed values are from a $2N + 4$ DOF system. The match in the amplitudes at the salient peaks is good, as also the salient frequencies in the spectral plots. Table 7 shows a comparison of experimental and analytical accelerations

obtained from the time records at various locations on the Sinusoidal track. Table 8 shows the same in case of roll and pitch rate.

Table 9 shows the comparison between experimental and analytical vertical acceleration responses at various locations on the APG track. Table 10 compares the experimental measurements of roll and pitch rates with those obtained from dynamic simulation. The comparison is good in all cases.

Transmissibility

Transmissibility is defined as the ratio of the maximum transmitted amplitude of vibration to the amplitude of the applied road input. Transmissibility helps in understanding the level of vibration isolation taking place between unsprung mass and sprung mass. In this study transmissibility has been studied in two stages: (i) from the wheel to the sprung mass CG and (ii) from the sprung mass CG to the driver's seat.

Stage I: Transmissibility from Wheel Station to Sprung Mass CG

In the first stage, acceleration response at wheel station 1 and sprung mass (hull) CG from experimental as well as dynamic simulation records are compared, both on Sinusoidal and APG tracks. Figure 14 shows the time record and spectrum of vertical acceleration measured on the Sinusoidal track at hull CG. Figure 15 shows the corresponding results from simulations on the same track at wheel station 1.

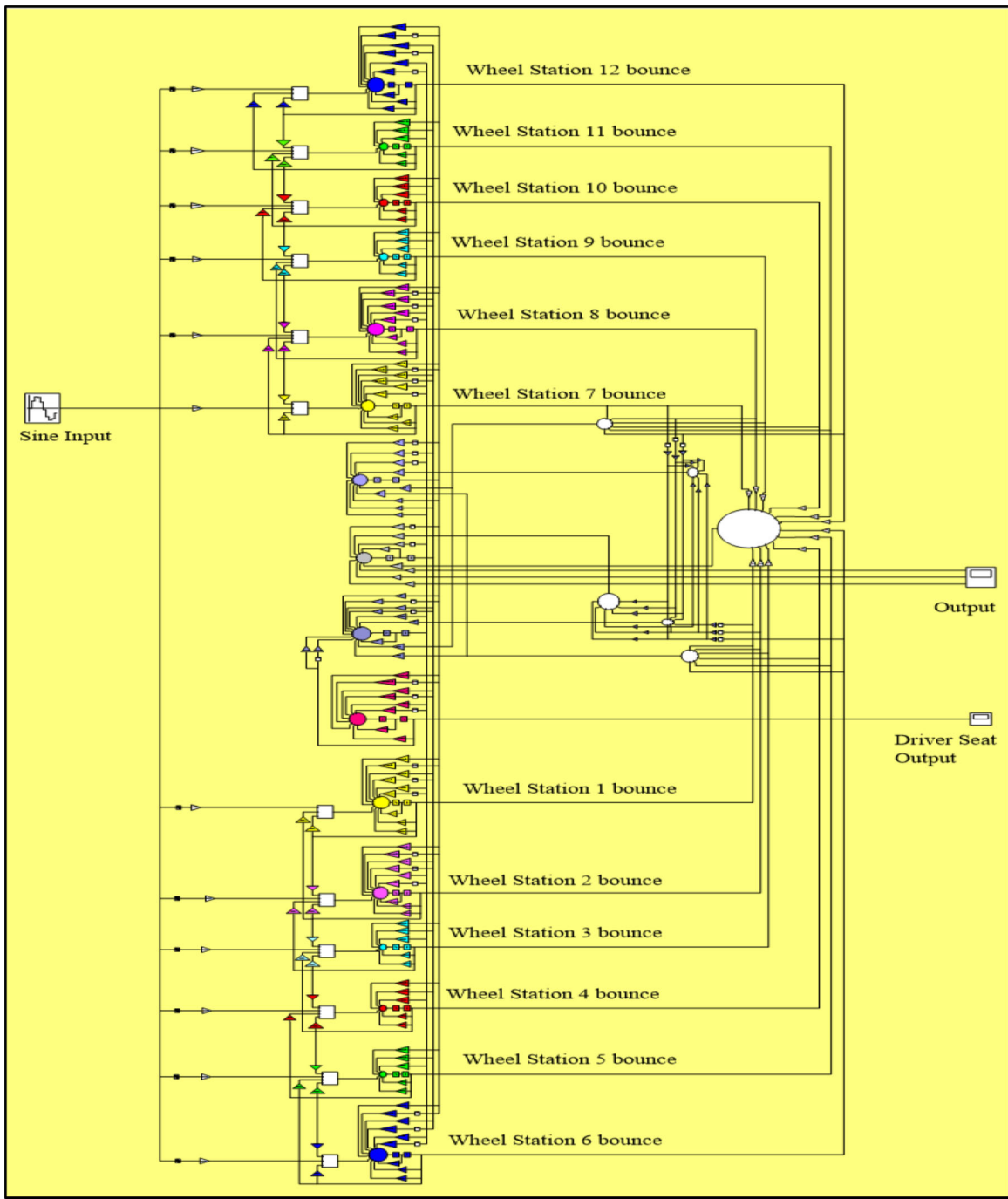


Fig. 10 Simulink 2N + 4 DOF model for ICV BMP-II on sinusoidal track

There are some high frequencies present in the experimental results in Fig. 14, which are not seen in the simulation. This is due to the imperfections in the physical Sinusoidal track, the troughs of which were covered with mud, giving rise to a spectrum with higher harmonics. Table 11 shows the peak to peak values of vertical acceleration response at hull CG and road wheel station 1 on Sinusoidal and APG tracks; these are further used to find out complete transmissibility from the road wheel to the driver's seat.

Stage II: Transmissibility from Sprung Mass CG to Driver's Seat

In the second stage, the study was carried out to measure vertical acceleration response at the sprung mass CG and driver's seat as shown in Fig. 16 for experiments on Sinusoidal track and Fig. 17 for simulation on the same. The ratio between vertical acceleration at driver's seat to acceleration at hull CG serves as an indicator of

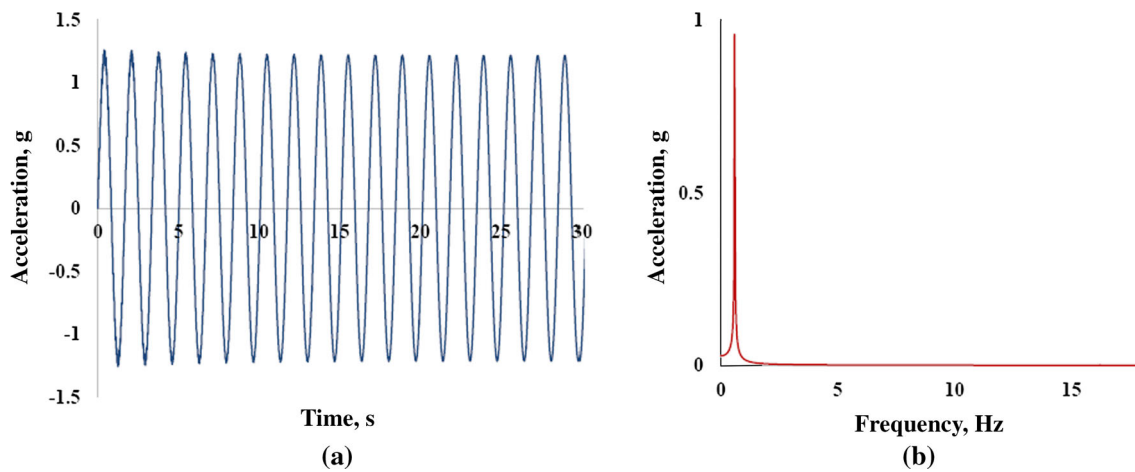


Fig. 11 **a** Time record of acceleration at wheel station 2 in vertical direction on a simulated Sinusoidal track. **b** Spectrum of acceleration at wheel station 2 in vertical direction on a simulated Sinusoidal track

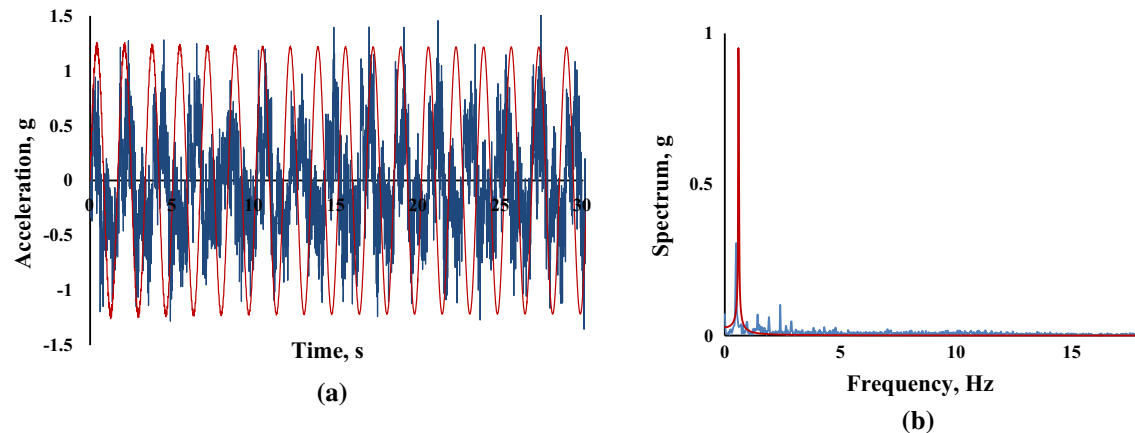


Fig. 12 **a** Time record of acceleration at wheel station 2 in vertical direction on Sinusoidal track. **b** Spectrum of acceleration at wheel station 2 in vertical direction on Sinusoidal track

Fig. 13 Time record of acceleration at wheel station 3 in vertical direction on APG track

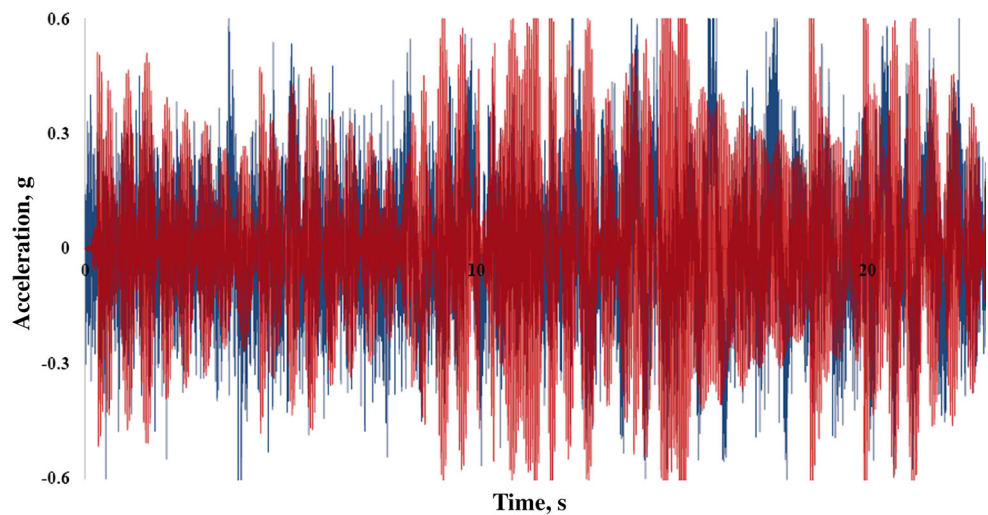


Table 7 Comparison of analytical and experimental response on Sinusoidal track

Location/direction	Experimental		Dynamic simulation	
	Peak to peak, g	RMS, g	Peak to peak, g	RMS, g
Wheel station 1/vertical	3.18	0.90	3.01	0.82
Wheel station 2/vertical	3.06	0.86	2.52	0.86
Wheel station 3/vertical	1.68	0.18	1.62	0.15
Wheel station 4/vertical	1.17	0.35	0.89	0.31
Wheel station 5/vertical	2.00	0.43	1.27	0.41
Wheel station 6/vertical	2.64	0.59	1.61	0.56
Driver seat/vertical	3.13	0.74	2.44	0.67
Hull CG/vertical	1.75	0.83	2.65	0.77

Table 8 Comparison of analytical and experimental pitch / roll rates on Sinusoidal track

Location/direction	Experimental		Dynamic Simulation	
	Peak to peak, degree/s	RMS, degree/s	Peak to peak, degree/s	RMS, degree/s
Hull CG/rolling	0.74	0.10	0.66	0.10
Hull CG/pitching	1.45	0.25	1.04	0.37

Table 9 Comparison of analytical and experimental acceleration responses on APG track

Location/direction	Experimental		Dynamic simulation	
	Peak to peak, g	RMS, g	Peak to peak, g	RMS, g
Wheel station 1/vertical	10.82	1.16	8.83	0.39
Wheel station 2/vertical	3.76	0.63	3.65	0.47
Wheel station 3/vertical	1.90	0.25	1.49	0.18
Wheel station 4/vertical	2.14	0.21	2.10	0.19
Wheel station 5/vertical	1.42	0.16	1.10	0.14
Wheel station 6/vertical	2.33	0.26	2.13	0.23
Driver seat/vertical	2.14	0.27	1.64	0.25
Hull CG/vertical	2.09	0.26	1.92	0.23

Table 10 Comparison of analytical and experimental pitch / roll rates on APG track

Location/direction	Experimental		Dynamic simulation	
	Peak to peak, degree/s	RMS, degree/s	Peak to peak, degree/s	RMS, degree/s
Hull CG/rolling	0.66	0.10	0.41	0.06
Hull CG/pitching	2.93	0.29	1.99	0.42

the effectiveness of the driver's seat cushion. Table 12 shows experimental and analytical peak to peak values of vertical acceleration response at hull CG and driver's seat on Sinusoidal and APG tracks; these responses were then used to find out total transmissibility.

Conclusions

The dynamic tests suggest that the torsion bar is an effective suspension system and has the ability to isolate most of the low frequency vibrations, the transmissibility from the road

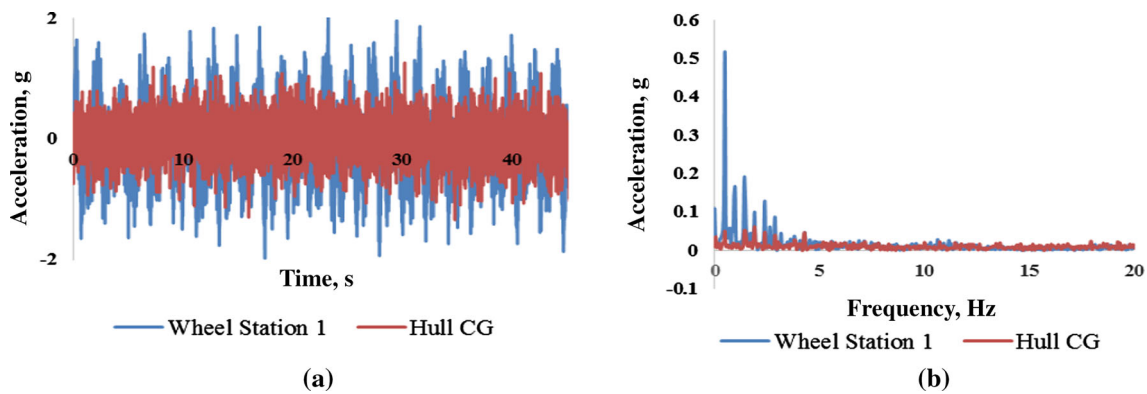


Fig. 14 **a** Time record of acceleration at hull CG and wheel station 1 on Sinusoidal track from measurement **b** Spectrum of acceleration at hull CG and wheel station 1 on Sinusoidal track from measurement

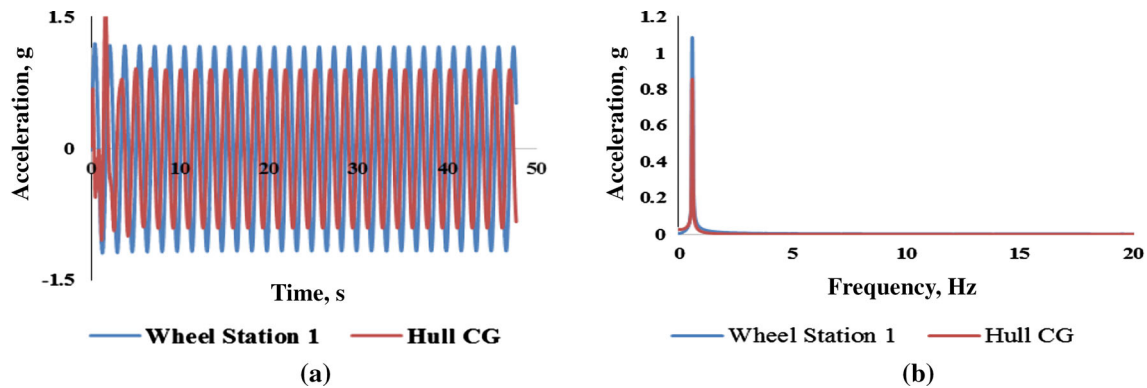


Fig. 15 **a** Time record of acceleration at hull CG and wheel station 1 on Sinusoidal track from simulation. **b** Spectrum of acceleration at hull CG and wheel station 1 on Sinusoidal track from simulation

Table 11 Transmissibility from road wheel to hull CG

Track	Experimental/dynamic simulation	Wheel station 1 Peak to peak	Hull CG Peak To Peak	Transmissibility = $\frac{\text{Acceleration at Hull}}{\text{Acceleration at Wheel}}$
Sinusoidal track	Experimental	4.01	2.58	0.64
	Simulation	2.39	1.86	0.78
APG track	Experimental	3.43	2.67	0.78
	Simulation	4.38	2.20	0.50

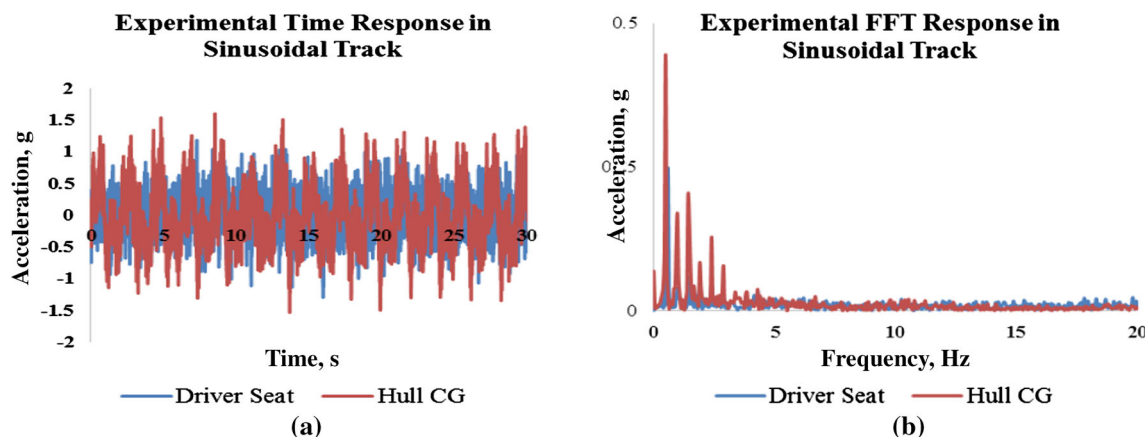


Fig. 16 **a** Time record of acceleration at hull CG and driver's seat on Sinusoidal track **b** Spectrum of acceleration at hull CG and driver seat on Sinusoidal track

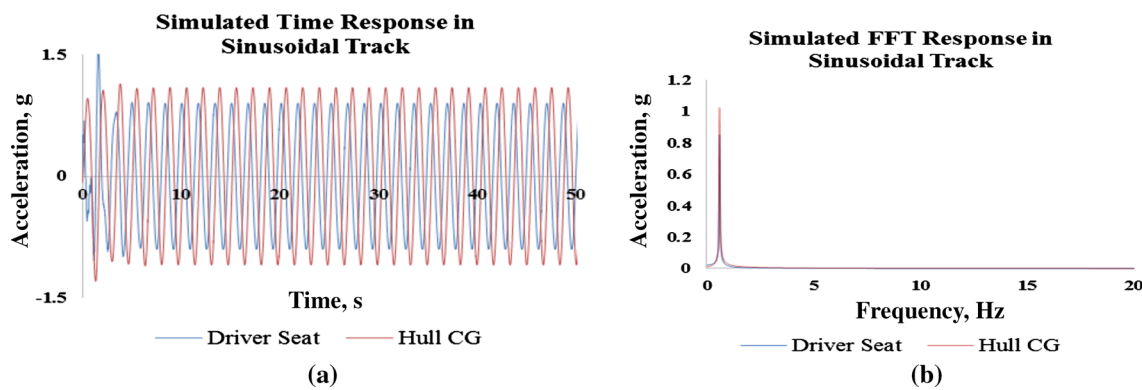


Fig. 17 **a** Time record of acceleration at hull CG and driver's seat on a simulated Sinusoidal track **b** FFT of acceleration at Hull CG and driver seat on a simulated Sinusoidal track

Table 12 Transmissibility from hull CG to driver's seat

Track	Experimental/simulation	Hull CG Peak to peak	Driver seat Peak to peak	Transmissibility = $\frac{\text{Output Amplitude}}{\text{Input Amplitude}}$
Sinusoidal track	Experimental	3.13	2.58	0.82
	Simulation	2.84	2.45	0.86
APG track	Experimental	3.12	1.74	0.56
	Simulation	2.20	1.62	0.73

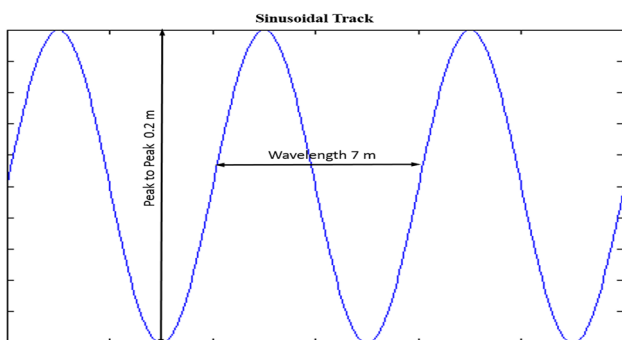
wheel to the hull being about 0.6. The same can be concluded from the simulation results. The dynamic force transmitted to the hull CG through the 12 torsion bar suspension systems was computed to be around 26,700 N and validated using measured values, with a very good match.

Acknowledgements The authors acknowledge the support received from Ordnance Factory, Medak and Combat Vehicles Research and Development Establishment, Chennai, India for conducting the experiments and would like to thank them. Further, necessary funding for the study was provided by IIT Madras.

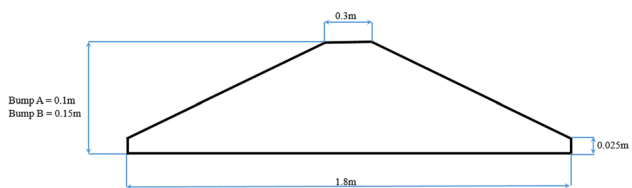
Funding Funding was provided by IIT Madras.

Appendix: Specifications of Sinusoidal and APG Track Profile

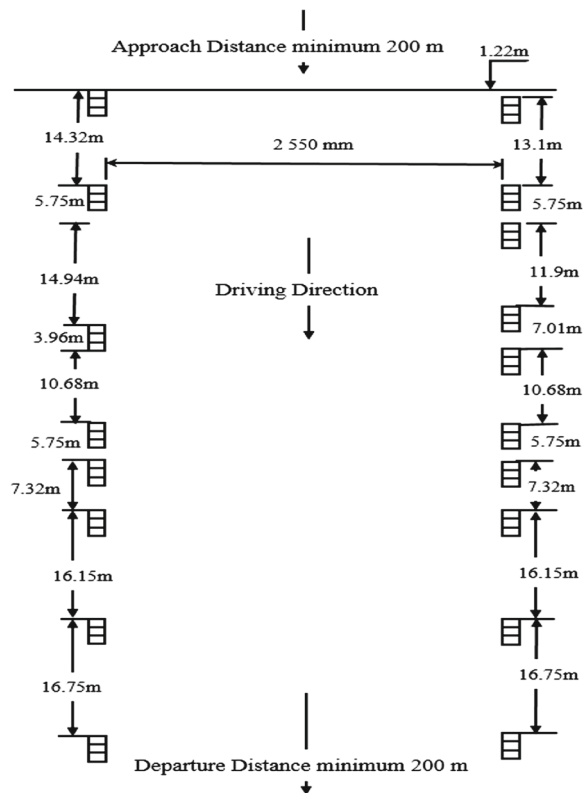
Sinusoidal Track Profile



APG Track Bumps



APG Track Profile



References

1. G.H. Hohl, Torsion-bar spring and damping systems of tracked vehicles. *J. Terramech.* **22**(4), 195–203 (1986)
2. S. Rakheja, M.F.R. Alfanso, S. Sankar, Dynamic analysis of tracked vehicles with trailing arm suspension and assessment of ride vibrations. *Int. J. Veh. Des.* **13**(1), 56–77 (1992)
3. A. Dhir, S. Sankar, Analytical track models for ride dynamic simulation of tracked vehicles. *J. Terramech.* **31**(2), 107–138 (1994)
4. A. Dhir, S. Sankar, Assessment of tracked vehicle suspension system using a validated computer simulation model. *J. Terramech.* **32**(3), 127–149 (1995)
5. C. Sujatha, A.K. Goswami, J. Roopchand, Vibration and ride comfort studies on tracked vehicle. *Int. J. Veh. Des.* **9**(3), 241–252 (2002)
6. J. Yamakawa, K. Watanabe, A spatial motion analysis model of tracked vehicles with torsion bar type suspension. *J. Terramech.* **41**(2), 113–126 (2004)
7. H. Baokun, Multibody model and simulation of the tracked vehicles, in *Proceedings of International Conference on Computer, Mechatronics, Control and Electronic Engineering (CMCE)*, pp. 200–202
8. Z.A. Kadir, M.A.M. Naiem, B. Bohari, K.A. Jalil, M.F.M. Yusoff, Validation of 2 dof tracked vehicle model due to road disturbance. *J. Mech. Eng.* **1**(3), 15–18 (2012)
9. A.M. Salem, T. Salahuddien, Evaluation of characteristics of tracked vehicle torsion bars. http://www.academia.edu/8651499/Evaluation_of_Characteristics_of_Tracked_Vehicles_Torsion_Bars3